

CORROSION OF STAINLESS STEEL TYPE 316L IN A SEEPAGE WATER DRIPPING ENVIRONMENT

Prepared for

**U.S. Nuclear Regulatory Commission
Contract NRC-02-07-006**

Prepared by

**H. Jung¹
T. Ahn²
T. Mintz¹**

**¹Center for Nuclear Waste Regulatory Analyses
San Antonio, Texas**

**²U.S. Nuclear Regulatory Commission
Washington, DC**

September 2011

ABSTRACT

This report documents the results of a previously unpublished set of experiments that evaluated the corrosion behavior of 316L stainless steel of nuclear grade under seepage water dripping conditions. Tests were conducted inside a chamber at a controlled temperature and relative humidity. Simulated seepage water was dripped on the test specimens at rates of 65 or 80 mL/day [2.20 or 2.71 oz/day] depending on the test temperature. Two batches of tests were conducted: (i) at 80 °C [176 °F] and 85 percent relative humidity and (ii) at 95 °C [203 °F] and 75 percent relative humidity. After the tests, the posttest specimens were examined with an optical microscope and salt deposits were analyzed in terms of chemical composition and phase. Finally, after cleaning the posttest specimens, weight loss was measured to calculate corrosion rates.

In all of the tested conditions, white deposits were observed on the posttest specimens. In the first batch of tests, the surfaces of the posttest specimens exhibited several corrosion pits after 37 day of dripping tests. The average corrosion rate was 27 nm/yr [1.06×10^{-6} in/yr] after 37 days. In the second batch at 95 °C [203 °F], pits were also present on the specimen surface and the surface was heavily corroded without passivation. After 67 days of dripping tests, the average corrosion rate was 930 nm/yr [3.66×10^{-5} in/yr]. Results of chemical and phase analyses of the salts and thermodynamic calculations indicate that the major composition was calcium carbonate and several other compositions were also precipitated, including magnesium carbonate, sodium (calcium) sulfate, sodium chloride, and silica.

CONTENTS

Section	Page
ABSTRACT	ii
FIGURES	iv
TABLES	v
ACKNOWLEDGMENTS	vi
1 INTRODUCTION	1-1
1.1 Background Information	1-1
1.2 Objective and Organization of the Report	1-2
2 EXPERIMENTAL DETAILS	2-1
2.1 Materials	2-1
2.2 Test Procedures	2-1
3 RESULTS AND DISCUSSION	3-1
3.1 First Batch of Tests at 80 °C [176 °F] and Relative Humidity of 85 Percent.....	3-1
3.2 Second Batch of Tests at 95 °C [203 °F] and Relative Humidity of 75 Percent	3-3
3.3 Salt Deposits Analysis	3-7
4 CONCLUSIONS.....	4-1
5 REFERENCES	5-1

FIGURES

Figure	Page
1-1	Range of Waste Package Temperature Versus Time Modeled for the Proposed Yucca Mountain Repository 1-3
1-2	Range of Relative Humidity Versus Time Modeled for the Proposed Yucca Mountain Repository 1-3
2-1	Experimental Setup for Dripping Test 2-2
2-2	Weight Losses of the Corroded Test Specimens Resulting From Repetitive Cleaning Cycles in an ASTM HNO ₃ Solution 2-3
3-1	Photos of Posttest Surfaces of 316L Stainless Steel After 37 Days of Dripping at 80 °C [176 °F] and 85 Percent Relative Humidity 3-2
3-2	Optical Micrographs of 316L Stainless Steel Surfaces After 37 Days of Dripping at 80 °C [176 °F] and 85 Percent Relative Humidity: 3-3
3-3	Surface Topography of 316L Stainless Steel Specimen after 37 Days of Dripping at 80 °C [176 °F] and 85 Percent Relative Humidity: (a) Optical Micrograph, (b) 3-D Laser Scan Profiles of the Pit Area, and (c) 2-D Profiles 3-4
3-4	Optical Micrographs of 316L Stainless Steel Surfaces after 67 Days of Dripping at 95 °C [203 °F] and 75 Percent Relative Humidity. 3-6
3-5	Energy-Dispersive X-ray Spectroscopy of the Salts Deposited on the 316L Stainless Steel Specimen Tested (a) at 80 °C [176 °F] and 85 Percent Relative Humidity and (b) at 95 °C [203 °F] and 75 Percent Relative Humidity. 3-9
3-6	X-ray Diffraction Spectra of Salts Deposited on the 316L Stainless Steel Specimens Tested (a) at 80 °C [176 °F] and 85 Percent Relative Humidity and (b)) at 95 °C [203 °F] and 75 Percent Relative Humidity. Also Shown Are the Reference Spectra of Salts That Best Match the Salt Deposit Spectra 3-10

TABLES

Table	Page
2-1	Chemical Composition of 316L Stainless Steel (in Weight Percent).....2-1
2-2	Chemical Composition of Simulated Seepage Water in This Study.....2-2
2-3	Test Matrix of 316L Stainless Steel Dripping Tests2-4
3-1	Corrosion Rates of 316L Stainless Steel After 37 Days of Dripping Test at 80 °C [176 °F] and 85 Percent Relative Humidity3-5
3-2	Corrosion Rates of 316L Stainless Steel After 67 Days of Dripping Test at 95 °C [203 °F] and 75 Percent Relative Humidity3-7
3-3	Elemental Composition of Salt Deposit on 316L Stainless Steel Specimens Tested (i) at 80 °C [176 °F] and 85 Percent Relative Humidity and (ii) at 95 °C [203 °F] and 75 Percent Relative Humidity (in Weight Percent):3-8

ACKNOWLEDGMENTS

This report describes work performed by the Center for Nuclear Waste Regulatory Analyses (CNWRA) and its contractors for the U.S. Nuclear Regulatory Commission (USNRC) under Contract No. NRC-02-07-006. The activities reported here were performed on behalf of the USNRC Office of Nuclear Material Safety and Safeguards, Division of High-Level Waste Repository Safety and Safeguards, Division of High-Level Waste Repository Safety. This report is an independent product of the CNWRA and does not necessarily reflect the view or regulatory position of the USNRC. The USNRC staff views expressed herein are preliminary and do not constitute a final judgment or determination of the matters addressed or of the acceptability of any licensing action that may be under consideration at USNRC.

The authors gratefully acknowledge K. Chiang for his technical review, D. Pickett for his programmatic review, L. Mulverhill for her editorial review, and A. Ramos for his administrative support. Special thanks to B. Derby, G. Bird, and G. Norman for their assistance in conducting experiments in this study.

QUALITY OF DATA, ANALYSES, AND CODE DEVELOPMENT

DATA: All CNWRA-generated original data contained in this report meet the quality assurance requirements described in the Geosciences and Engineering Division Quality Assurance Manual. Sources for other data should be consulted for determining the level of quality for those data. All data and calculations related to this report have been recorded in CNWRA Scientific Notebooks 899 and 1081 (Jung, et al., 2011a,b).

ANALYSES AND CODES: None.

References

Jung, H., B. Derby, and G. Bird. "Seepage Water Dripping Test for Alloy 22 in the Repository Relevant Environments." Scientific Notebook No. 899. San Antonio, Texas: CNWRA. pp. 1-108. 2011a.

_____. "Seepage Water Dripping Test for Alloy 22 in the Repository Relevant Environments." Scientific Notebook No. 1081. San Antonio, Texas: CNWRA. pp. 1-7. 2011b.

1 INTRODUCTION

This report is part of the knowledge management activities for the U.S. Nuclear Regulatory Commission high-level waste repository program. The report provides previously undocumented results from recent corrosion tests that used weight loss measurements and surface analysis to evaluate the corrosion behaviors of stainless steel type 316L waste package inner shell material under seepage water dripping conditions. The corrosion experiments were conducted by dripping simulated seepage water in two batches with varying temperature and relative humidity: (i) at 80 °C [176 °F] and 85 percent relative humidity and (ii) at 95 °C [203 °F] and 75 percent relative humidity. The corrosion rates of stainless steel specimens were estimated by measuring weight loss of the posttest specimens. The surfaces of the specimens were examined with an optical microscope, and the salts deposited on the specimens were also analyzed using energy dispersive x-ray spectroscopy and x-ray diffraction.

1.1 Background Information

316L stainless steel of nuclear grade (UNS S31603) is a candidate material for inner structural supports and radiation shielding in disposal waste packages (DOE, 2008). Traditionally, stainless steel has been studied in various disposal programs across the world as a reference waste package material in various geological settings (Kursten, et al., 2004). For interim storage, stainless steel may be used as a canister material for the storage cask. In this case, in particular, in a chloride-containing environment, stress corrosion cracking is a potential degradation mechanism of canister failure due to formation of salt deposits and the deliquescence process (EPRI, 2005). The dripping water tests with formation of salt deposits in this study are likely to provide important information on the salt deliquescence and corrosion behavior of a stainless steel canister in this environment. Usually, the material design of stainless steel of nuclear grade follows the ASME Boiler and Pressure Vessel Code and the thickness of the material ranges from centimeters to tens of centimeters [inches to feet], depending on the applications.

The high corrosion resistance of 316L stainless steel is attributed, in part, to the presence of a passive oxide film that protects against fast corrosion. In the event of deterioration or loss of the passivity of stainless steel at earlier times and subsequent fast corrosion, weaker mechanical strength or breach by localized corrosion or stress corrosion cracking could occur. Therefore, it is important to determine the long-term general corrosion rates and susceptibility to localized corrosion and stress corrosion cracking of 316L stainless steel under various service conditions. This report presents test results of general corrosion and localized corrosion. Most corrosion data used in disposal and storage applications were obtained from immersion experiments to develop the model abstraction for the general corrosion rate and susceptibility to localized corrosion. However, in an unsaturated disposal environment, or in a dry storage environment (EPRI, 2006), the corrosion environment is likely to be either dripping seepage water or a humid chloride-containing atmosphere. In both cases, the corrosion temperatures are expected to be higher than ambient values due to radioactivity decay. Therefore, it is expected that salt deposits can occur by seepage water evaporation in a geologic repository, seawater evaporation in a marine environment, and/or airborne salt accumulation in a dry storage system.

Figures 1-1 and 1-2 show the modeled ranges of temperature and relative humidity versus time for all waste packages in the proposed Yucca Mountain repository, accounting for uncertainty of host-rock thermal conductivity and percolation flux (Sandia National Laboratories, 2008). During the first 10,000 years, the waste package temperatures could have a wide range from a peak of 203 °C [398 °F] to room temperature. In the time period of 1,500 to 10,000 years, there

is a possibility that one or a few waste package outer containers could fail and allow seepage water to contact the stainless canister. The average temperature during this period is predicted to be about 95 to 60 °C [203 to 140 °F], and the average relative humidity could range from approximately 75 to 95 percent. These ranges of modeled temperature and relative humidity were selected for the experimental conditions in this study.

Under storage conditions, details of the relative humidity on the hot canister have not been assessed, although atmospheric relative humidity is tabulated at various coastal areas (EPRI, 2006). Some considerations have been presented on the relative humidity on hot canister surfaces (Shirai, et al., 2011a,b). Compared to the data presented in Shirai, et al. (2011a,b), relative humidity on the hot canister surface is likely similar to the lower portion of Figure 1-2 at higher temperatures.

Recent model development work on general corrosion and localized corrosion of stainless steel for repository application suggests a low bound of the general corrosion rate of 0.01 µm/year [3.94×10^{-7} in/yr] and a high bound of 3 µm/yr [1.18×10^{-4} in/yr] in an oxidizing environment with oxidizers, mainly oxygen (He, et al., 2011). This variation is due to a range of pH of 1.9 to 13 and temperatures of 30–80 °C [86–176 °F]. In the presence of salt deposits, the temperature for aqueous conditions will increase above the water boiling point (Shirai, et al., 2011a,b; Caseres and Mintz, 2010) due to salt deliquescence. He, et al. (2011) also summarized pitting susceptibility quantitatively in terms of the probability that a waste package can fail by localized corrosion.

1.2 Objective and Organization of the Report

The objective of the present work is to document the results of recent corrosion tests that used weight loss measurements and surface analysis to evaluate the corrosion behavior of 316L stainless steel under seepage water dripping conditions. The present work conducted corrosion tests to assess the persistence of the passive film and to measure the corrosion rate. The persistence of the passive film was assessed by determining susceptibility to localized corrosion (primarily pitting), and the general corrosion rate was determined by weight loss measurement. Note that this report presents preliminary results and longer term corrosion tests are warranted for conclusive results.

This report consists of four chapters: introduction, experimental details, results and discussion, and conclusions. This chapter briefly describes the corrosion behaviors of stainless steel and its applications as a storage or disposal canister. Environmental conditions, including temperature and relative humidity, are also discussed in this chapter. Experimental conditions in this study are provided in Chapter 2, including details of test samples, test solutions, and test procedures. Results of experiments and analyses are discussed in Chapter 3, including surface and salts analyses, weight loss measurements, and corrosion rates calculation. Chapter 4 provides the study conclusions.

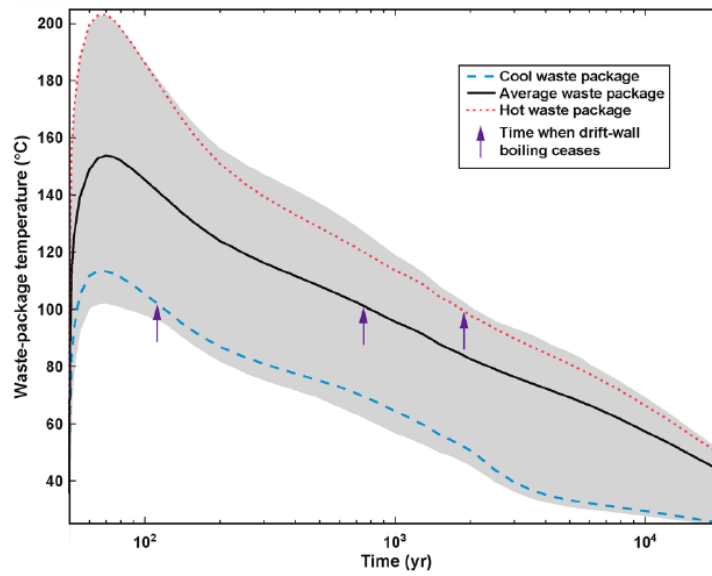


Figure 1-1. Range of Waste Package Temperature Versus Time Modeled for the Proposed Yucca Mountain Repository (Sandia National Laboratories, 2008)

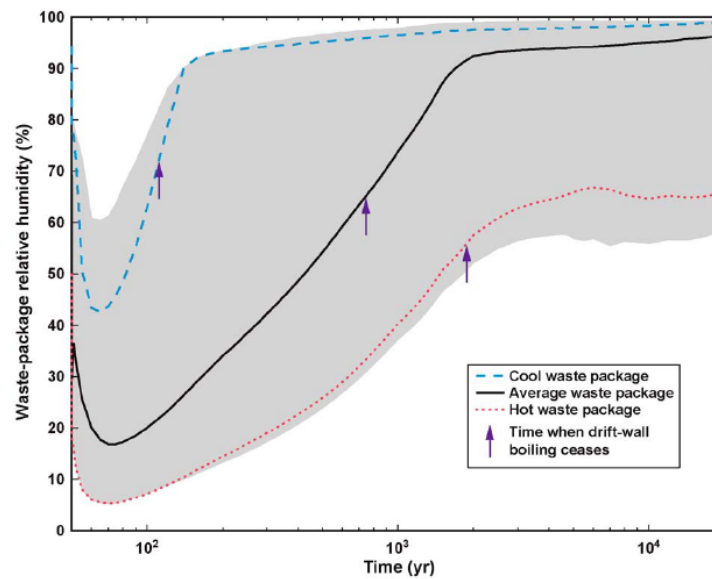


Figure 1-2. Range of Relative Humidity Versus Time Modeled for the Proposed Yucca Mountain Repository (Sandia National Laboratories, 2008)

2 EXPERIMENTAL DETAILS

2.1 Materials

The samples used for the tests were disk-shaped stainless steel type 316L plate metal. The chemical composition of the stainless steel type 316L (HT 7470663) samples is shown in Table 2-1. The samples had a diameter of 5.08 cm [2.0 in] and a thickness of 0.635 cm [0.25 in]. The specimens were polished up to a 2,000-grit sand paper and 2,000 diamond paste for the final finish, rinsed and ultrasonically cleaned in deionized water and acetone, and dried.

2.2 Test Procedures

The dripping corrosion tests of stainless steel were conducted inside a chamber with controlled temperature and relative humidity as shown in Figure 2-1. Each test specimen was set on a 3.4-cm [1.3-in] outer diameter polytetrafluoroethylene cylinder spacer. The polytetrafluoroethylene cylinders with the test specimens were placed inside a polytetrafluoroethylene tray in the chamber. The top of the dripping tubes was located about 10 cm [4 in] above the test specimen. The dripping water was simulated seepage water with the chemical composition shown in Table 2-2. Dunn, et al. (2006) used the same composition to represent neutral-type seepage waters in experiments to evaluate the effect of environmental conditions on the performance of Alloy 22 waste package material. The water was pumped from a reservoir outside of the chamber through polytetrafluoroethylene tubing into the chamber and allowed to drip on the test specimen. The temperature and relative humidity were controlled and maintained to be constant through the testing periods. The temperature and relative humidity near the test specimens were monitored by using additional measurement probes from the outside. The probes of the thermocouple and humidity gauge were extended to be located close to the test specimens. Because the chamber's temperature and humidity sensors were located at the edge on the ceiling inside the chamber, it was necessary to confirm the actual temperature and relative humidity directly exposed to the test specimens that was located on the chamber floor.

The posttest specimens were observed under an optical microscope for pitting or other possible corrosion features. Surface deposits and/or surface oxides on the posttest specimens were analyzed with energy-dispersive x-ray spectroscopy and x-ray diffraction. Weight loss measurement was used to measure the corrosion rates of stainless steel. In all of the tested conditions for Alloy 22, white deposits were observed on the surface of posttest specimens. After carefully removing and collecting the surface deposits, the specimens were first rinsed with deionized water and then chemically cleaned multiple times in a nitric acid (HNO₃) solution {100 mL [3.4 oz] diluted to 1,000 mL [34 oz] deionized water} in accordance with the procedures recommended in ASTM G1-03 (ASTM International, 2003). The specimens were immersed

Fe*	Cr*	Ni*	Mo*	Cu*	Co*	Si*	Al*	Mn*	V*	P*	S*	C*	N*
Bal†	16.48	10.30	2.11	0.32	0.19	0.53	0.005	1.38	0.058	0.028	0.0006	0.021	0.023
*Fe—iron; Cr—chromium; Ni—nickel; Mo—molybdenum; Cu—copper; Co—cobalt; Si—silicon; Al—aluminum; Mn—manganese; V—vanadium; P—phosphorous; S—sulfur; C—carbon; N—nitrogen †Bal—balance													

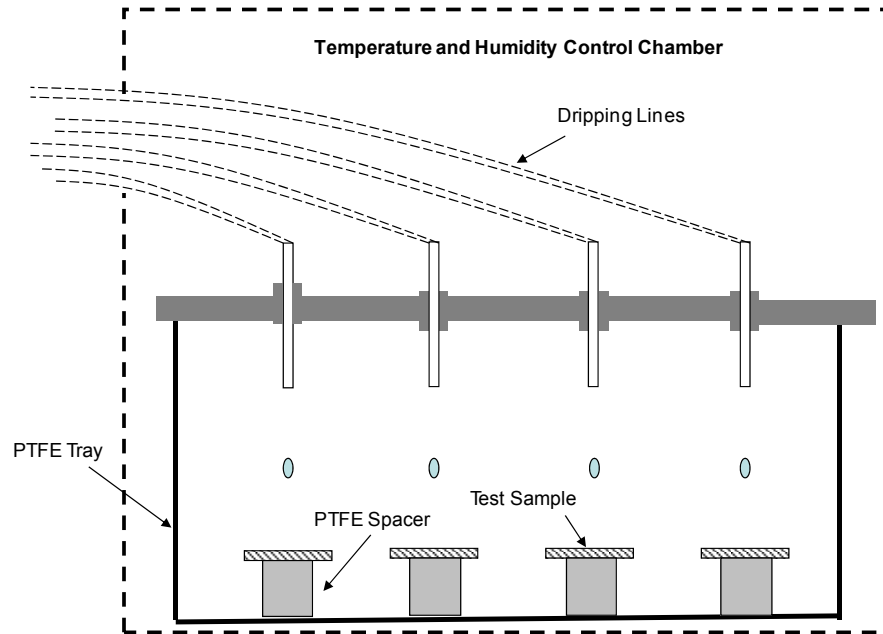


Figure 2-1. Experimental Setup for Dripping Test

Table 2-2. Chemical Composition of Simulated Seepage Water in This Study

Ion	Na ⁺	K ⁺	Mg ²⁺	Ca ²⁺	Cl ⁻	SO ₄ ²⁻	NO ₃ ⁻	HCO ₃ ⁻	CO ₃ ²⁻
mol/L (M)	1.5 × 10 ⁻²	1.7 × 10 ⁻⁴	4.9 × 10 ⁻⁴	9.9 × 10 ⁻⁴	7.7 × 10 ⁻⁴	7.0 × 10 ⁻³	1.5 × 10 ⁻³	1.7 × 10 ⁻³	1.7 × 10 ⁻⁵

for 20 minutes at 60 °C [140 °F]. Then, the specimens were ultrasonically cleaned in acetone and dried. Before measuring the weight loss of the posttest specimens, the cleaned surface was observed by optical microscope to confirm the absence of any remaining deposits on the surface. The weight change was measured using a microbalance with a precision of ± 2.5 × 10⁻⁵ g [8.82 × 10⁻⁷ oz]. Figure 2-2 shows a typical plot for weight loss measurements as a function of the number of cleanings. The four test specimens were exposed at 95 °C [203 °F] and 75 percent relative humidity for 67 days. The weight loss plateaued after two or three

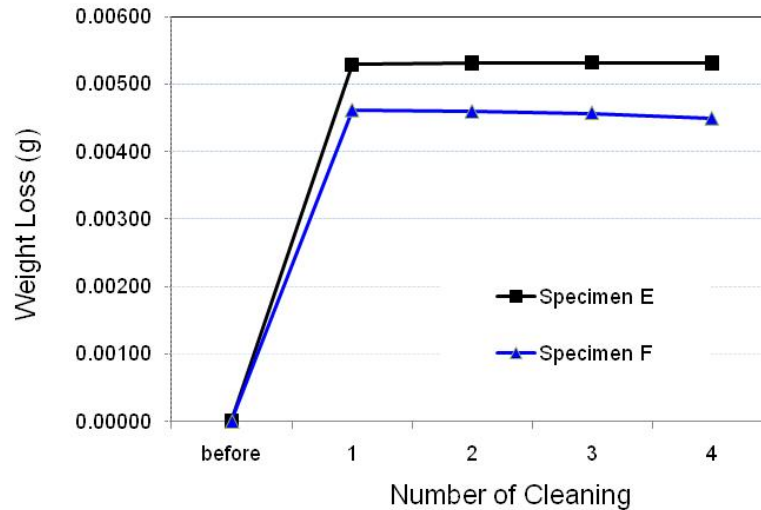


Figure 2-2. Weight Losses of the Corroded Test Specimens Resulting From Repetitive Cleaning Cycles in an ASTM HNO₃ Solution (ASTM International, 2003). The Weight Loss After the Third Cycle of Cleaning Was Used in the Weight Loss Analysis.

cycles of cleaning. Therefore, the weight losses after the third cycle of cleaning were used to calculate the corrosion rate in accordance with the equation defined in ASTM G1-03 (ASTM International, 2003). Table 2-3 shows the test matrix of stainless steel for two batches: (i) at 80 °C [176 °F] and 85 percent relative humidity and (ii) at 95 °C [203 °F] and 75 percent relative humidity. The table also provides information on the test duration and sample identification number for each batch. The temperature and humidity selected were close to the mean values of modeled temperature and relative humidity at times of ~2,500, and ~1,500 years for the first and second batches, respectively, as shown in Figures 1-1 and 1-2. The water dripping rates for each set were selected based on the modeled seepage water flow rates for each repository time and were adjusted a focused flow to be equivalent to the test specimen size, as discussed in Jung, et al. (2011).

To evaluate the depth of pitting, the posttest stainless steel samples were analyzed with a laser profilometer. The laser profilometer is a noncontact, fully automatic imaging system with a depth resolution (z axis of the machine) of 0.5 μm [1.97×10^{-5} in] and lateral surface resolution of 1 μm [3.94×10^{-5} in] (x and y axes). The laser profilometer uses a laser-optical displacement sensor and signal conditioning electronics to measure the vertical distance on a material. The laser used is a helium-neon laser operating a wavelength of 632.8 nm [2.49×10^{-5} in]. The sensor uses the optical triangulation principle where a visible, modulated point of light is projected onto the sample surface. The diffusive part of the reflection of this point of light is focused onto a charged couple device array. The intensity of the beam provides information about the vertical distance. Laser scans of surface morphology were conducted for all four samples. The scan lateral resolution was set at 5 μm [1.97×10^{-4} in].

Table 2-3. Test Matrix of 316L Stainless Steel Dripping Tests			
Temperature and Relative Humidity	Water Dripping Rate	Test Duration	Specimen Identification
80 °C [176 °F] and 85 Percent Relative Humidity	80 mL/day [2.71 oz/day]	37 Days	A, B, C, and D
95 °C [203 °F] and 75 Percent Relative Humidity	65 mL/day [2.20 oz/day]	67 Days	E and F

3 RESULTS AND DISCUSSION

This section summarizes and discusses the results of experiments and analyses of stainless steel, including weight loss measurements and corrosion surface morphologies. In addition, salt deposits formed on the posttest specimens were characterized in terms of chemical composition and phases using energy dispersive spectroscopy and x-ray diffraction.

3.1 First Batch of Tests at 80 °C [176 °F] and Relative Humidity of 85 Percent

Figure 3-1 shows optical photos of the posttest specimens after 37 days of dripping tests at 80 °C [176 °F] and relative humidity of 85 percent. Most of the surface area on the front upper side subjected to water dripping was covered with white salt deposits. The white deposits were also observed on the lower back side, particularly the outside area of the polytetrafluoroethylene-spacer-covered inner area as seen in Figure 3-1.

Optical Microscopy

After removing the salt deposits followed by sample cleaning with HNO₃ solution, the specimens were examined with an optical microscope. Figure 3-2 shows typical morphologies of the corroded surface of stainless steel. After 37 days of dripping tests, as shown in Figure 3-2, corrosion pits were observed throughout the areas exposed to the dripping water for all tested specimens. Many small-sized pits {about 1 μm [3.94×10^{-5} in]} were also present. Caseres and Mintz (2010) also observed salt deposit formation and localized corrosion (i.e., pitting) on 304 stainless steel. In these tests by Caseres and Mintz (2010), 304 stainless steel was exposed to different chloride deposits, including a simulated sea salt, sodium chloride, and magnesium chloride deposits. The 304 stainless steel with the various salt deposits was exposed to different atmospheric conditions, including 50 °C [122 °F] at 65 percent relative humidity, 50 °C [122 °F] at 50 percent relative humidity, and 50 °C [122 °F] at 40 percent relative humidity. Under all of these conditions, pitting was observed for the samples exposed to simulated sea salt and magnesium chloride. Pitting was not observed on the samples exposed to sodium chloride, because the relative humidity used for the testing was not high enough to cause the salt to deliquesce. The pitting depth was not measured for these tests. One additional test was conducted for 304 stainless steel exposed to a simulated sea salt deposit at 65 °C [122 °F] at 70 percent relative humidity. Large pits were observed to form on the samples exposed to this environment. The pits were measured with laser profilometry, which provided a corrosion rate on the order of 4.5 mm/yr [0.180 in/yr].

Surface Topography

The observed pits were further analyzed by using laser profilometry to estimate the pit depth. Figure 3-3(a) shows a typical pit morphology of the corroded surface of stainless steel exposed to dripping conditions. As can be seen from both the three-dimensional and two-dimensional profiles in Figure 3-3(b) and 3-3(c), respectively, the pit has a width of roughly 150 μm [5.91×10^{-3} in] and a depth of roughly 40 μm [1.58×10^{-3} in]. These results are similar to those observed from optical microscopy.



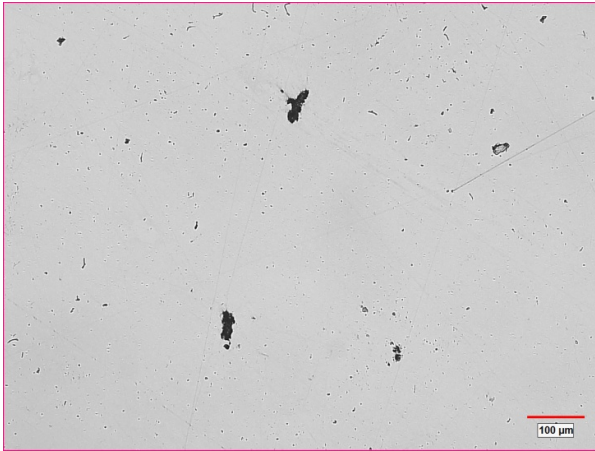
Figure 3-1. Photos of Posttest Surfaces of 316L Stainless Steel After 37 Days of Dripping at 80 °C [176 °F] and 85 Percent Relative Humidity

Corrosion Rate

Corrosion rates of stainless steel specimens were calculated using Eq. (3-1) per ASTM G1-03 (ASTM International, 2003), and results are listed in Table 3-1

$$\text{Corrosion Rate [nm/yr]} = (8.76 \times 10^{10} \times \Delta w) / (\rho \times A \times t) \quad (3-1)$$

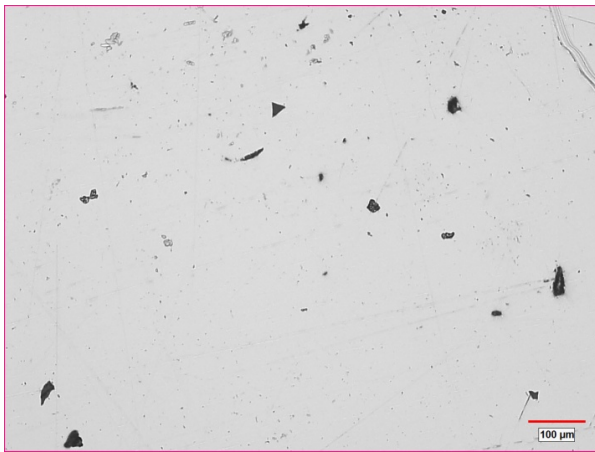
[where Δw : weight loss (g), ρ : stainless steel density {7.98 g/cm³ [0.29 lb/in³]}, A: exposed surface area {36.25 cm² [5.62 in²]}, and t: exposed time (hours)]. The exposed surface of 36.25 cm² [5.62 in²] is the sum of the areas, including the upper front side of 20.27 cm² [3.14 in²], the edge area of 4.78 cm² [0.74 in²], and the wetted back side of 11.19 cm² [1.73 in²]. Because a part of the lower back side, except the area inside the polytetrafluoroethylene cylinder spacer, was wetted with the dripped water as seen in Figure 3-1, this wetted area of 11.19 cm² [1.73 in²] was included in the exposed surface area.



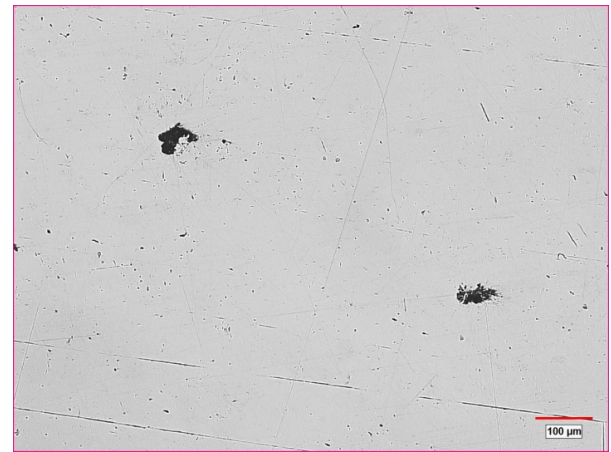
Specimen A



Specimen B



Specimen C



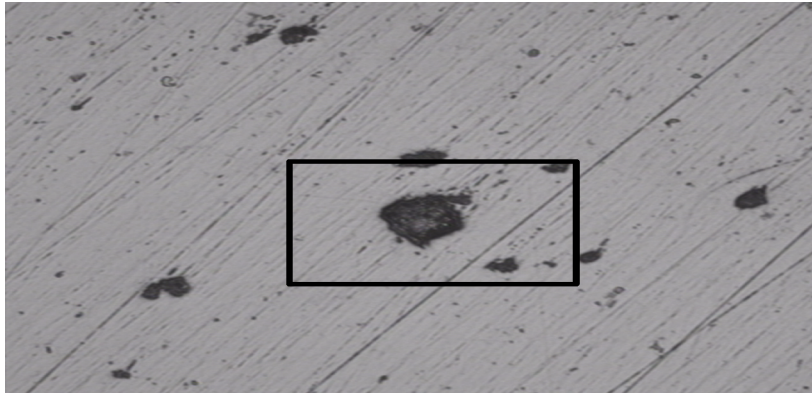
Specimen D

Figure 3-2. Optical Micrographs of 316L Stainless Steel Surfaces After 37 Days of Dripping at 80 °C [176 °F] and 85 Percent Relative Humidity

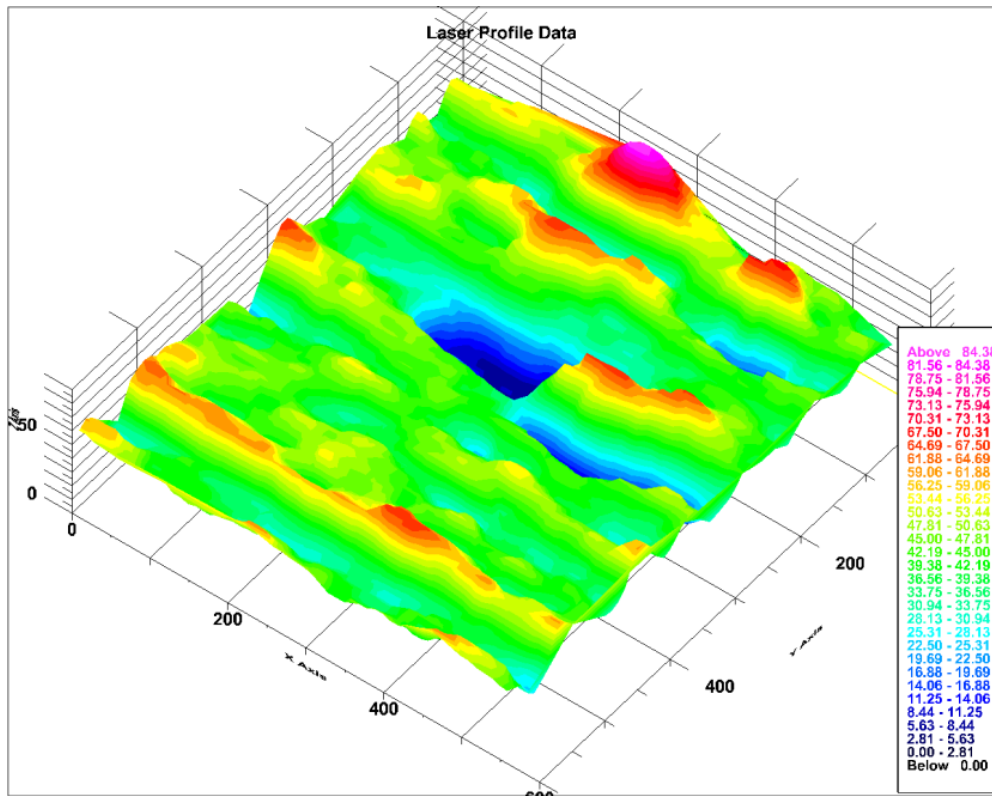
As seen in Table 3-1, all samples exhibited weight loss and the amount of loss increased with test time. After 37 days, the corrosion rate ranged from 10 to 41 nm/yr [3.94×10^{-7} to 1.61×10^{-6} in/yr] and the average rate was 27 nm/yr [1.06×10^{-6} in/yr] with the standard deviation of 13.4 nm/yr [5.28×10^{-7} in/yr]. This average rate is close to a low bound of corrosion rate of 10 nm/yr [3.94×10^{-7} in/yr] for stainless steel in the literature, as discussed in Chapter 1.

3.2 Second Batch of Tests at 95 °C [203 °F] and Relative Humidity of 75 Percent

Similar to the observations on stainless steel from the first batch, the posttest stainless steel specimens were covered with white deposits after 67 days of dripping tests at 95 °C [203 °F]

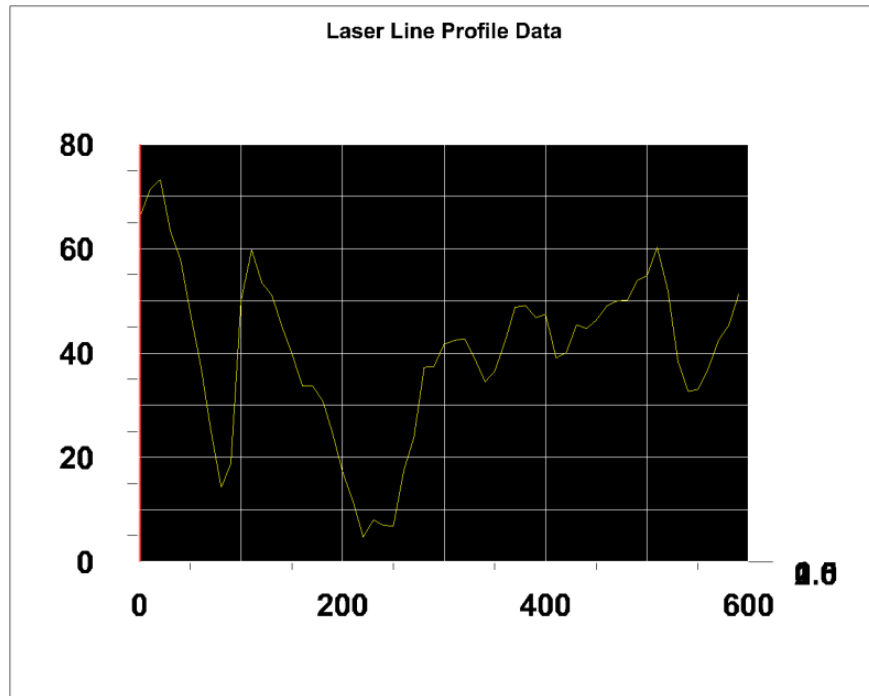


(a)



(b)

Figure 3-3. Surface Topography of 316L Stainless Steel Specimen after 37 Days of Dripping At 80 °C [176 °F] and 85 Percent Relative Humidity: (a) Optical Micrograph, (b) 3-D Laser Scan Profiles of the Pit Area, and (c) 2-D Profiles. Note: the Square Box in (a) Indicates the Laser Scanning Area. The Units in (b) and (c) Indicate x, y, and z axes Are in Micrometers.



(c)

Figure 3-3 (continued). Surface Topography of 316L Stainless Steel Specimen after 37 Days of Dripping At 80 °C [176 °F] and 85 Percent Relative Humidity: (a) Optical Micrograph, (b) 3-D Laser Scan Profiles of the Pit Area, and (c) 2-D Profiles. Note: the Square Box in (a) Indicates the Laser Scanning Area. The Units in (b) and (c) Indicate x, y, and z axes Are in Micrometers.

Table 3-1. Corrosion Rates of 316L Stainless Steel After 37 Days Dripped at 80 °C [176 °F] and 85 Percent Relative Humidity				
Specimen Identification	Initial Weight (g)	Weight Loss (g)	Corrosion Rate (nm/yr)*	Average Corrosion Rate ± Standard Deviation (nm/yr)†
A	47.92718	0.00003	10	27 ± 13.4
B	47.66421	0.00007	24	
C	48.06729	0.00012	41	
D	47.99737	0.00010	34	

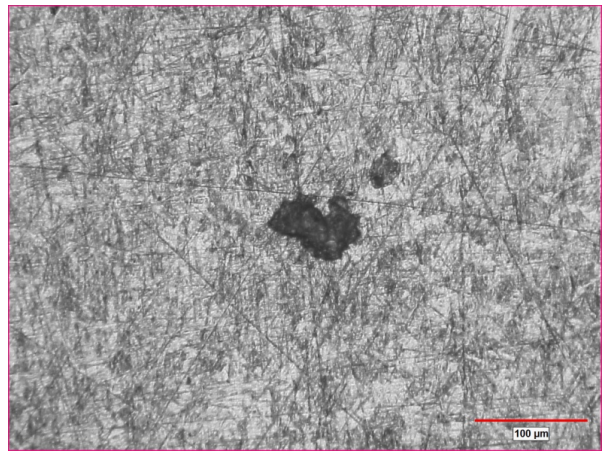
*1 nm/yr = 3.94 × 10⁻⁸ in/yr

and relative humidity of 75 percent (not shown here). After removing the deposits, as seen in Figure 3-4, the stainless steel surface exhibited several corrosion pits and the surface was heavily corroded. There was also evidence of grain boundary attack [see Figure 3-4(b) and 3-4(c) on specimen F]. With a slightly higher test temperature of 95 °C [203 °F] compared to the first batch, it appeared there was active dissolution without passivation under the test condition.

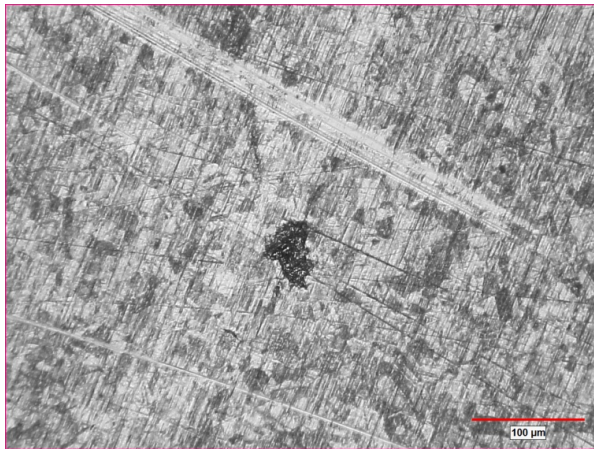
This nonpassivation of stainless steel resulted in a relatively high corrosion rate as shown in the results in Table 3-2, which lists calculated corrosion rates with weight losses after 67 days of tests. The average corrosion rate was 931 nm/yr [3.54×10^{-5} in/yr], and this rate was much higher than that measured at 80 °C [176 °F] in the first batch. The higher test temperature led to a higher corrosion rate.



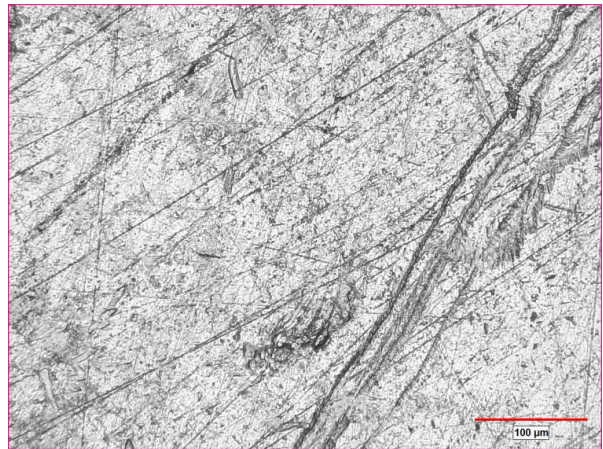
Specimen E (Front Side)



Specimen F (Front Side)



Specimen F (Front Side)



Specimen F (Back Side Center Area)

Figure 3-4. Optical Micrographs of 316L Stainless Steel Surfaces after 67 Days of Dripping at 95 °C [203 °F] and 75 Percent Relative Humidity

Specimen Identification	Initial Weight (g)	Weight Loss (g)	Corrosion Rate (nm/yr)*	Average Corrosion Rate ± Standard Deviation (nm/yr)*
E	48.00047	0.00532	1,002	931 ± 99.9
F	47.87168	0.00457	861	

*1 nm/yr = 3.94 × 10⁻⁸ in/yr

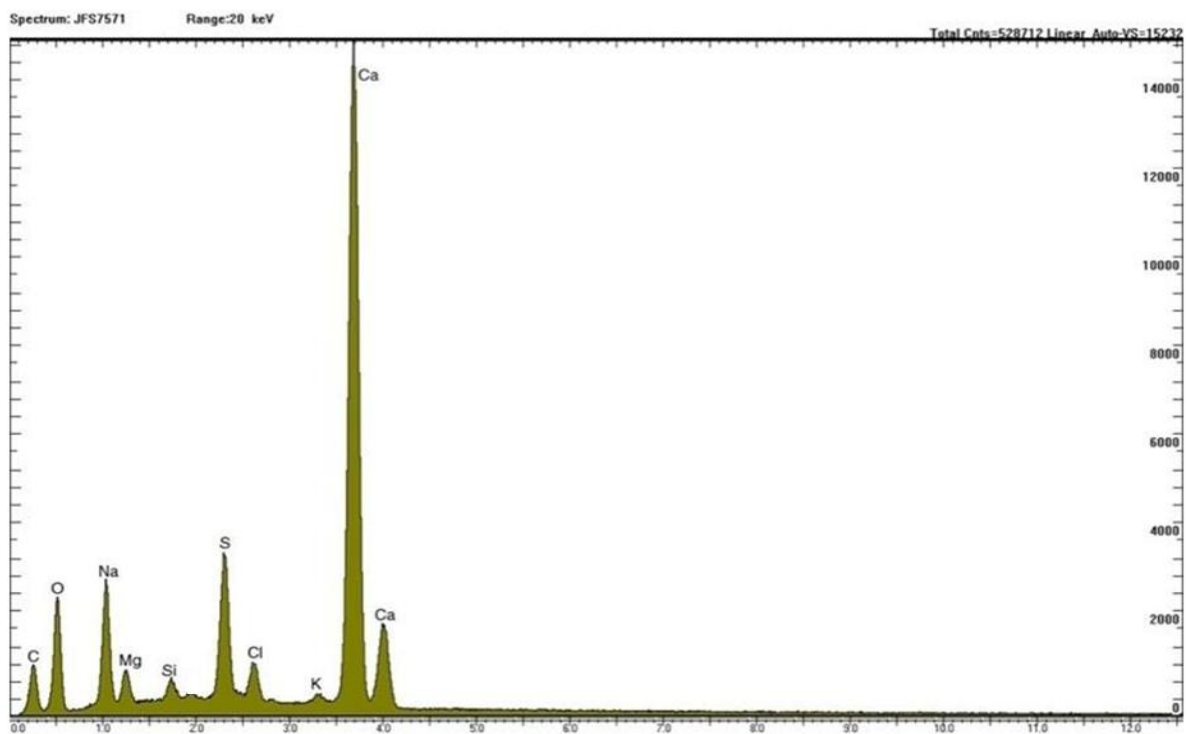
3.3 Salt Deposits Analysis

The chemical compositions and phases of the salts deposited on the stainless steel specimens were analyzed using energy dispersive x-ray spectroscopy and x-ray diffraction analysis. Energy dispersive x-ray spectroscopy was used to determine the elemental composition of the corrosion products, whereas x-ray diffraction analysis was used to determine the phase composition. Energy dispersive x-ray spectroscopy analysis was carried out using a Noran Voyager M3105 system. X-ray diffraction analysis was carried out using a Siemens Kristalloflex 805 with D500 Goniometer. The salts present in the corrosion products were identified by comparing the x-ray diffraction analysis spectra of the samples with reference spectra of different salts in a database. Note that x-ray diffraction analysis using the goniometer for this study has a detection limit of about 5 weight percent to identify a phase composition.

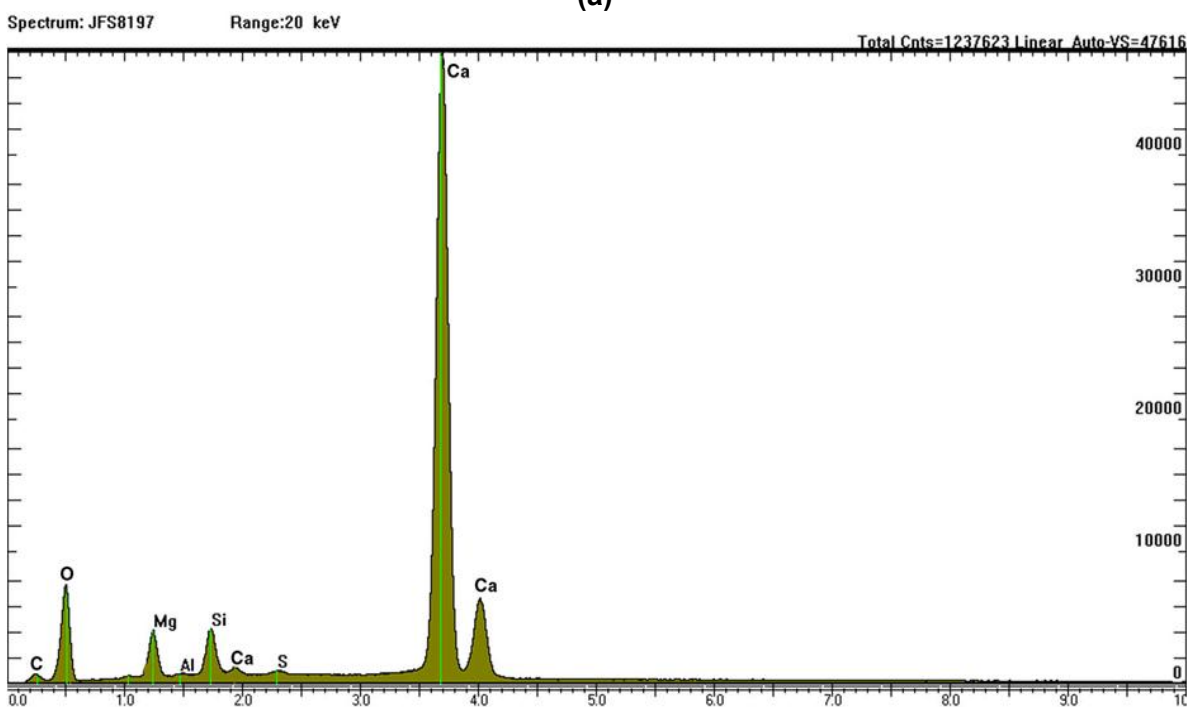
The energy dispersive x-ray spectroscopy analysis results of salt deposits from the first and second batches are shown in Table 3-3 and Figure 3-5. Figure 3-5 shows that the white deposits consist of calcium, carbon, oxygen, sodium, magnesium, aluminum, silicon, sulfur, and chloride. The higher concentrations of calcium, carbon, and oxygen suggest that the white deposit is primarily calcium carbonate, deposited from the evaporation of the dripping water. This salt was also confirmed from the x-ray diffraction analysis data shown in Figure 3-6, which indicates that the salts are dominantly calcium carbonate. Sodium, magnesium, sulfur, and chloride came from the dripping water. Aluminum and silicon are likely from residual deposits from the specimen surface preparation process before the test and/or possibly from the stainless steel matrix by dissolution. In particular, a significant amount of silicon (more than 5 weight percent) appeared on the salt formed in the second batch compared to the silicon concentration in the first batch.

Previous thermodynamic calculation results from an OLI Analyzer Studio evaporation simulation (OLI Systems Inc., 2010) indicated the possible formation of calcium carbonate, magnesium carbonate, sodium sulfate, and sodium-calcium sulfate for the salts formed by evaporation under the two batch test conditions (Jung, et al., 2011). Based on the energy dispersive x-ray spectroscopy results, silicate compounds and sodium chloride also could be present in the salt deposit but in amounts less than the detection limit of the x-ray diffraction analysis.

Table 3-3. Elemental Composition of Salt Deposit on 316L Stainless Steel Specimens Tested (i) at 80 °C [176 °F] and 85 Percent Relative Humidity and (ii) at 95 °C [203 °F] and 75 Percent Relative Humidity (in Weight Percent)		
Element	(i) 80 °C [176 °F] and 85 Percent Relative Humidity	(ii) 95 °C [203 °F] and 75 Percent Relative Humidity
Na	16.81	0.75
Mg	4.00	6.91
Al	—	0.54
Si	1.51	5.18
S	10.45	0.44
Cl	3.25	—
Ca	63.09	86.18
Total	100.00	100.00



(a)



(b)

Figure 3-5. Energy-Dispersive X-ray Spectroscopy of the Salts Deposited on the 316L Stainless Steel Specimen Tested (a) at 80 °C [176 °F] and 85 Percent Relative Humidity and (b) at 95 °C [203 °F] and 75 Percent Relative Humidity

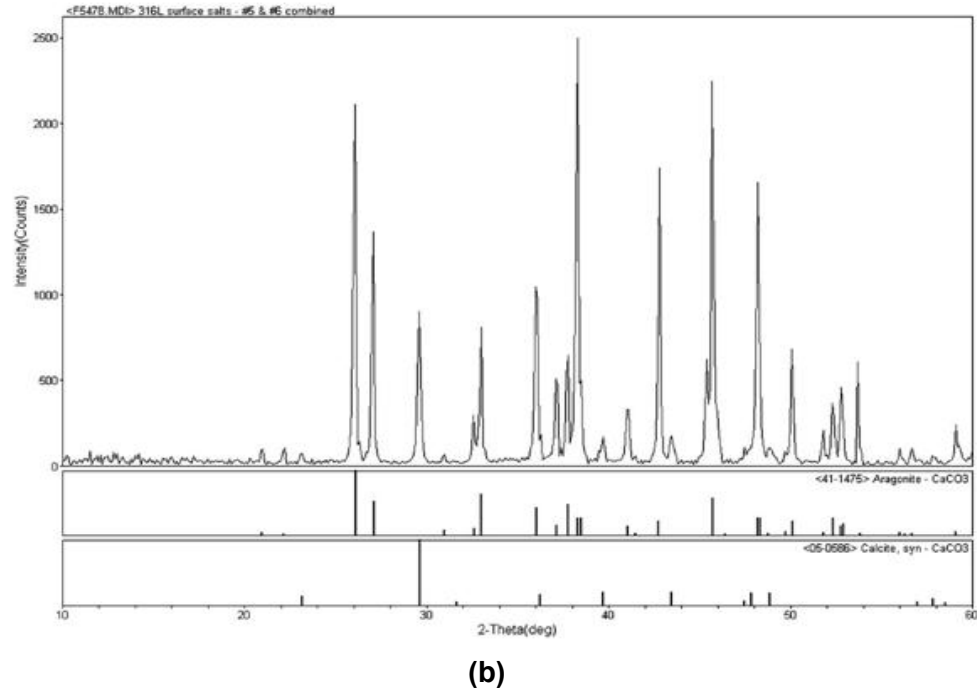
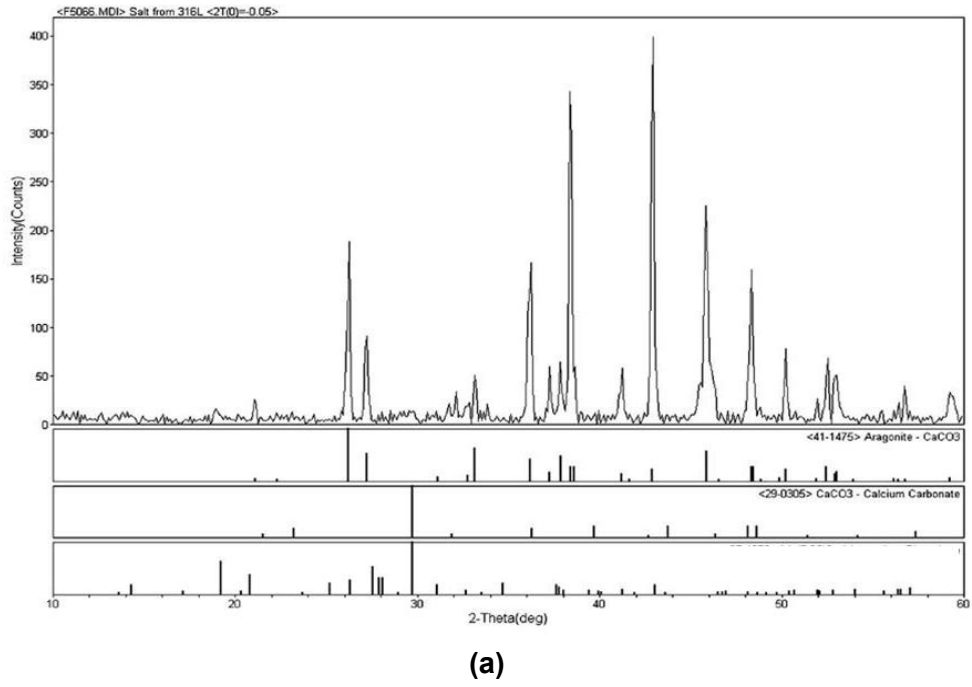


Figure 3-6. X-ray Diffraction Spectra of Salts Deposited on the 316L Stainless Steel Specimens Tested (a) at 80 °C [176 °F] and 85 Percent Relative Humidity and (b) at 95 °C [203 °F] and 75 Percent Relative Humidity. Also Shown Are the Reference Spectra of Salts That Best Match the Salt Deposit Spectra.

4 CONCLUSIONS

In this report, the corrosion behavior of stainless steel type 316L was evaluated under seepage water dripping conditions. The main conclusions from this study follow.

- In the first batch of tests at 80 °C [176 °F] and 85 percent relative humidity, the surfaces of the posttest specimens exhibited several corrosion pits. After 37 days of dripping tests, the corrosion rate ranged from 10 to 41 nm/yr [3.94×10^{-7} to 1.61×10^{-6} in/yr] and the average rate was 27 nm/yr [1.06×10^{-6} in/yr]. This rate is close to a low bound of 10 nm/yr [3.94×10^{-7} in/yr] for stainless steel obtained from immersion tests in the literature.
- In the second batch of tests at 95 °C [203 °F] and 75 percent relative humidity, pits were also present on the specimen surface and the surface was heavily corroded. There was also evidence of grain boundary attack. It appeared there was active dissolution without passivation. After 67 days of dripping tests, the average corrosion rate was 930 nm/yr [3.54×10^{-6} in/yr] and this rate was much higher than that measured at 80 °C [176 °F] in the first batch. The higher test temperature led to a higher corrosion rate.
- Results of chemical and phase analyses of the salts and thermodynamic calculations indicate that the major composition was calcium carbonate and several other compositions were possibly precipitated, including magnesium carbonate, sodium (calcium) sulfate, sodium chloride, and silica.

5 REFERENCES

- ASTM International. "Preparing, Cleaning, and Evaluating Corrosion Test Specimens." ASTM G1-03. West Conshohocken, Pennsylvania: ASTM International. 2003.
- Caseres, L. and T.S. Mintz. NUREG/CR-7030, "Atmospheric Stress Corrosion Cracking Susceptibility of Welded and Unwelded 304, 304L, and 316L Austenitic Stainless Steels Commonly Used for Dry Cask Storage Containers Exposed to Marine Environments." Washington, DC: NRC. 2010.
- DOE. DOE/RW-0573, "Yucca Mountain Repository License Application." Rev. 0. ML081560400. Las Vegas, Nevada: DOE, Office of Civilian Radioactive Waste Management. 2008.
- Dunn, D.S., Y.-M. Pan, X. He, L.T. Yang, and R.T. Pabalan. "Evolution of Chemistry and Its Effects on the Corrosion Engineered Barrier Materials." The 30th Symposium on the Scientific Basis for Nuclear Waste Management. Fall Meeting, Boston, Massachusetts, November 27–December 1, 2006. Pittsburg, Pennsylvania: Materials Research Society. 2006.
- EPRI. "Climatic Corrosion Considerations for Independent Spent Fuel Storage Installations in Marine Environments." EPRI 1013524. Palo Alto, California: Electric Power Research Institute. 2006.
- _____. "Effects of Marine Environments on Stress Corrosion Cracking of Austenitic Stainless Steels." EPRI 1011820. Palo Alto, California: EPRI. 2005.
- He, X., O. Pensado, T. Ahn, and P. Shukla. "Model Abstraction of Stainless Steel Waste Package Degradation." Proceedings of 2011 International Radioactive Waste Management Conference (IHLRWMC), Albuquerque, New Mexico, April 10–14, 2011. Paper No. 3460. La Grange Park, Illinois: American Nuclear Society. 2011.
- Jung, H., X. He, T. Ahn, T. Mintz, and R. Pabalan. "Corrosion of Alloy 22 and Titanium Alloys Under Seepage Water Dripping Conditions." San Antonio, Texas: Center for Nuclear Waste Regulatory Analyses. 2011.
- Kursten, B., E. Smailos, I. Azkarate, L. Werme, N.R. Smart, and G. Santarini. "COBECOMA, State-of-the-Art Document on the Corrosion Behavior of Container Materials." Contract No. FIKW-CT-20014-20138. Final Report. Brussels, Belgium: European Commission. 2004.
- OLI Systems, Inc. "A Guide to Using OLI Analyzer Studio Version 3.1." Morris Plains, New Jersey: OLI Systems, Inc. 2010.
- Sandia National Laboratories. "Multiscale Thermohydrologic Model." ANL-EBS-MD-000049. Rev. 03, ADD 02 ERD 1. Las Vegas, Nevada: Sandia National Laboratories. 2008.
- Shirai, K., M. Wataru, and T. Saegusa. "Long-Term Containment Performance Test of Metal Cask." Proceedings of 2011 International Radioactive Waste Management Conference (IHLRWMC), Albuquerque, New Mexico, April 10–14, 2011. Paper No. 3332. La Grange Park, Illinois: American Nuclear Society. 2011a.

Shirai, K., J. Tani, T. Arai, M. Wataru, H. Takeda, and T. Saegusa. "SCC Evaluation of Multi-Purpose Canister." Proceedings of 2011 International Radioactive Waste Management Conference (IHLRWMC), Albuquerque, New Mexico, April 10–14, 2011. Paper No. 3333. La Grange Park, Illinois: American Nuclear Society. 2011b.